SOILS AND FOUNDATIONS Vol. 49, No. 4, 631–650, Aug. 2009
Japanese Geotechnical Society

INTERPRETATION OF INTERNATIONAL PARALLEL TEST ON THE MEASUREMENT OF G_{max} USING BENDER ELEMENTS

SATOSHI YAMASHITA[i], TAKAYUKI KAWAGUCHI[ii], YUKIO NAKATA[iii], TAKEKO MIKAMI[iv], TERUYUKI FUJIWARA[v] and SATORU SHIBUYA[vi]

ABSTRACT

This report summarizes the results of international parallel test on the measurement of the elastic shear modulus at very small strains, G_{max}, using bender elements which was carried out from 2003 to 2005 by technical committee, TC29 (Stress-strain and Strength Testing of Geomaterials) of the International Society of Soil Mechanics and Geotechnical Engineering. The purpose was to evaluate the consistency of the bender element test results obtained by applying the exactly similar test material as well as the test method besides identifying the various existing hardware and software being used in this test. It was decided that the domestic TC29 group of Japanese Geotechnical Society (TC29-JGS) was expected to lead this international co-operation. By 2005, reports of the test results were obtained from 23 institutions from 11 countries. This report has been prepared by TC29-JGS taking a leading role from the beginning. A standard test method is proposed here in order to obtain more accurate data from the bender element test by examining various test methods adopted at different institutions worldwide and the effects of various factors on the test results.

Key words: bender element, international parallel test, laboratory test, secondary wave velocity, shear modulus, small strain, test procedure (**IGC**: D6/D7)

INTRODUCTION

Parameters (shear modulus G and damping h) required for the dynamic response of geomaterials due to dynamic loads, such as traffic loads, earthquakes and machine vibrations, are being evaluated by using laboratory tests and from in-situ seismic tests. It is now commonly known that stress-strain behaviour of geomaterials is non-linear and G value decreases but damping ratio increases with the increase in strain level. In order to evaluate this non-linearity, stress-strain responses due to monotonic or cyclic loadings are evaluated by using triaxial or torsional shear testing machines, commonly known as static loading methods. On the other hand, applying wave motions in the test specimens and observing their behaviour at resonance including free oscillation time, such as resonant column apparatus, are other kinds of evaluation methods, called as vibration test methods. Besides them, some methods, such as ultrasonic pulse test, bender element (BE) test etc., which calculate G_{max} at very small strains based on the wave velocity, are called as pulse transmission techniques.

Among these testing methods described in previous paragraphs, the static loading and vibration methods are standardized in each nation (e.g., JGS, BS and ASTM), and are being used worldwide. However, the testing procedures are not unified. In addition, the effects of the sampling method, the preparation method and the test procedure on the test results are unclear. Therefore, sharing the information internationally with the application of test results into practice, and preparing international guidelines were needed. TC29 was formed under such a background in 1994.

In the last ten years, TC29 has been active with the aim of improving laboratory shear testing apparatus and test methods, generalization of the mechanical properties of different types of geomaterials and their engineering applications. In doing that, four international conferences, IS-Hokkaido (1994), Geotechnique Symposium (1997), IS-Torino (1999) and IS-Lyon (2003), have been sponsored until recently along with the publication of proceedings and a summary book (Tatsuoka et al., 2001).

One of the prime missions of TC29 is to optimize and internationalize the laboratory test apparatus and test methods being used in characterizing deformation behaviour of geomaterials. TC29 has already conducted two international parallel tests in the past by using the same soil and the same test method (Toki et al., 1995; Yamashita et

[i] Professor, Kitami Institute of Technology, Japan (yamast@mail.kitami-it.ac.jp).
[ii] Associate Professor, Hakodate National Collage of Technology, Japan.
[iii] Associate Professor, Yamaguchi University, Japan.
[iv] Oyo Corporation, Japan.
[v] Geo-Research Institute, Japan.
[vi] Professor, Kobe University, Japan.
The manuscript for this paper was received for review on June 12, 2008; approved on June 8, 2009.
Written discussions on this paper should be submitted before March 1, 2010 to the Japanese Geotechnical Society, 4-38-2, Sengoku, Bunkyo-ku, Tokyo 112-0011, Japan. Upon request the closing date may be extended one month.

al., 2001).

The BE test has become quite popular in the last ten years due to its simplicity, low cost and non-destructive nature. The test is not only limited to the leading countries for laboratory tests, but has extended globally via foreign graduates from these countries. However, the process of defining the travel distance of shear wave, time of travel, the input wave type, input frequency, hardware and software for removing the noise and many other factors differ in each laboratory. Most often, these factors are decided on personal judgments rather than guided by procedures. To take up this issue seriously, TC29 has started international parallel test on BE in 2003 as one of its main activities.

Under the aforementioned background, the purpose of international parallel test on the BE was: i) to grasp the present condition of hardware/software being utilized in the BE test, ii) to strictly evaluate the consistency of test results from this test by using the same material and test procedures, and iii) to produce the original concept and international test guidelines for measuring shear modulus, G_{max} of different geomaterials. Having abundant backup data and track record, it was decided that the domestic TC29 committee of Japan, TC29-JGS takes the leading role for its execution.

INTERNATIONAL PARALLEL TEST

Test Specifications

Test specifications (*see* APPENDIX) were published on September 2003 at the 3rd Symposium on the Deformation Behaviour of Geomaterials (IS-Lyon'03), which was held in Lyon, France. Regarding the test material, Toyoura sand was purchased at once by TC29-JGS and distributed to the participating institutions including a nozzle for sample preparation. Here, the reasons for selecting the Toyoura sand as test material and air-pluviation method as the test method were: i) the past parallel tests using laboratory test equipment were conducted with this material (Tatsuoka et al., 1986; Toki et al., 1986; Miura et al., 1994), ii) the same sand was used for the parallel tests performed to evaluate the deformation behaviour (Toki et al., 1995), and iii) the previous international simultaneous test by TC-29 (Yamashita et al., 2001) also used the same test material. In addition, the large amount of accumulated test data on Toyoura sand in Japan as well as in many other countries worldwide ascertained ample opportunities to compare the results with past records.

The reason for selecting air pluviation technique for sample preparation was also due to the past record of being used in international parallel tests. In principle, JGS 0542-2000 (JGS, 2000) were followed for specimen preparation as well as for testing.

It was decided to test the specimen at relative densities of 50% and 80%. However, in order to obtain a relative density, it was necessary to calculate the maximum and minimum density ($\rho_{d\,max}$ and $\rho_{d\,min}$) and the results could differ among the participated institutions. To overcome this difficulty, members of TC29-JGS had performed the tests beforehand to evaluate $\rho_{d\,max}$ and $\rho_{d\,min}$ and the average value of required dry density was supplied to the institutions. Figure 1 shows the obtained results and the gradation of sand used for testing.

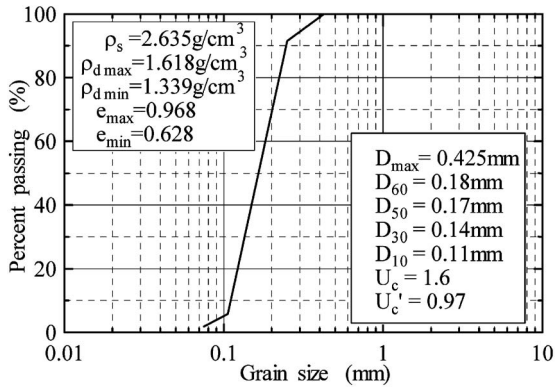

Fig. 1. Grain size of Toyoura sand

Participating Laboratories

The international parallel test was formally started by dispatching Toyoura sand and the nozzle for test to the participating institutions before March, 2004. Finally, report of the test result was prepared in September, 2005 based upon the submissions from 23 institutions worldwide. Table 1 shows the list of the participating institutions. The participating institutions consisted of 15 from Asia (Japan-11, China-1 and Korea-1), 9 from Europe (France-2, Italy-2, Finland-1, Netherlands-1, Portugal-1, Romania-1 and UK-1) and one from North America (Canada-1). By comparing the participated international institutions in the present and previous parallel test organized by TC29 (Yamashita et al., 2001), which was just 19 institutions from 6 countries (Japan-11, Greece-1, Italy-4, Korea-1, Portugal-1 and Spain-1), it is quite understandable that BE test is spreading worldwide and being quite popular.

Test Apparatus and Test Conditions

Table 2 enlists the details on test apparatus, specimen size and number of tests at different participating laboratories. It is to be noted here that Lab. No. in this table does not match with Table 1. The number of different types of test equipments, triaxial testing device (TX) − 17, consolidation (OM) and direct shear test equipment (DS) that use stiff metal container − 5, resonant column apparatus (RC) − 2 (including one torsional shearing (TS) apparatus), shows that triaxial device was primarily used. Regarding the specimen size in triaxial test, diameters of 50 mm and 70 mm totalled almost 80%. There were two cases where diameter above 100 mm was used. When examined for the ratio H/D, it was above 1.0 and equalled 2.0 in triaxial and resonant column method tests. In contrast, H/D was relatively small in consolidation and direct shear test equipments, where the specimens were put inside stiff metal containers.

Table 1. Participating laboratories

No.	Names: Affiliation	Country
1	Dr. D. Wijewickreme: University of British Columbia	Canada
2	Dr. Y.-g. Zhou: Zhejiang University	China
3	Dr. T. Länsivaara: Tampere University of Technology	Finland
4	Dr. C. Dano: Research Institute in Civil and Mechanical Engineering	France
5	Dr. H. Geoffroy and Dr. A. Ezaoui: ENTPE	France
6	Prof. D. C. F. Lo Presti and Dr. D. Androne: Technical University of Turin	Italy
7	Dr. R. Castellanza and Dr. C. Zambelli: Technical University of Milan	Italy
8	Mr. N. Takehara: Tokyo Soil Research Co., Ltd.	Japan
9	Prof. J. Kuwano and Dr. Tay: Tokyo Institute of Technology	Japan
10	Dr. T. Ogino: Akita University	Japan
11	Dr. Y. Nakata: Yamaguchi University	Japan
12	Mr. T. Fujiwara: Geo-Resurch Institute	Japan
13	Mr. K. Nishida: Hokkaido University	Japan
14	Mr. M.K. Mostafa: Osaka City University	Japan
15	Prof. J. Koseki: Institute of Industrial Science, University of Tokyo	Japan
16	Dr. T. Kawaguchi: Hakodate National College of Technology	Japan
17	Dr. S. Yamashita: Kitami Institute of Technology	Japan
18	Dr. Y. Mohri and Dr. T. Lohani: National Research Institute of Agricultural Engineering	Japan
19	Prof. D.-S. Kim: Korea Advanced Institure of Science and Technology	Korea
20	Dr. E. d. Haan: GeoDelft	Netherlands
21	Dr. C. Ferreira: University of Porto	Portugal
22	Dr. A. Cristian: National Center for Seismic Risk Reduction	Romania
23	Dr. A. Takahashi: Imperial College London	UK

On categorizing according to saturation condition, there were total of 60 tests on dry specimen and 45 with saturated specimen, thus making 105 in total. The relatively large number of tests on dry specimen could be due to simple test condition without necessitating saturation. However, there is another difficulty in accurate specimen volume change measurement when tested dry because it either needs double cell type arrangement or needs lateral strain measurements. In the tests performed, it was mostly found that volume change of dry specimen was simply taken as three times that the axial strain. The tests on dry specimens may also cause the difficulty in identifying the shear wave arrival time due to a near-field-effect (NFE) that goes up when the distance between the bender pairs decreases. It is reported that NFE are mainly influenced by P-wave signals that reach the receiving end before true shear wave signal (e.g., Brignoli et al., 1996; Arroyo et al., 2006), so that waveforms due to P-wave components may mask the true S-wave arrival. In particular, as the propagation velocity of the P-wave is much slower and the difference in propagation velocity of the P-wave and S-wave is smaller in dry specimen than saturated specimen, there is a high possibility that NFE is higher in dry specimens.

Regarding the stress condition at consolidation, isotropic stress state was followed in 55 test cases, which is more than half of the total. Tests under K_0 conditions were performed in consolidation or direct shear apparatus using a stiff container. There was one case that used triaxial apparatus (No. 5) but K_0 condition was not obtained by controlling the lateral stress so that no lateral strain was developed. In this test, a hard cylindrical Perspex glass was used to restrain the side displacement, which was principally similar to an oedometer or a direct shear device, and was put in the OM category.

Specifications of Bender Elements

Table 2 also plots the specifications of BEs that were used in the tests. The dimensions and signs are as shown in Fig. 2. Information on the thickness of epoxy coating t_c and the total thickness t are inscribed wherever available. Where there are no reports or unclear, columns are left blank.

Figure 3 shows a typical example of a BE set up. Here, the BE is a bimorph electric actuator that polarizes in the direction of thickness. Two ceramic elements are bonded together with a flexible shim of metal such as nickel acting as an electrode. In general, the material of the piezo-electric device was Lead Zirconium Titanate ($Pb(Ti.Zr)O_3$), called PZT. When electric voltage is applied on a bimorph piezo-electric element, one of the layer shrinks and the other extends due to piezoelectric effect, ultimately producing a bend in a whole element. On the other hand, when deformation is applied, the piezoelectric transducer generates a voltage. By using this property of the BE, either of the elements installed in a cap or pedestal are applied with electric voltage to generate shear waves and the element at the other end receives the signal enabling the measurement of shear wave velocity in the soil element.

In all the tests performed here, BE transducers were entirely made of PZT wherever the reporting was done. On observing the size, the length L_t of 12–20 mm, the width W of 10–12 mm and the thickness t of 0.5–1.0 mm was used. Thickness of waterproofing insulation, such as epoxy coating t_c seemed to be 0.5 mm in general.

There are two different ways of electric wirings to activate such piezo-electric devices to transmit or receive a shear wave, namely parallel type and series type. In a parallel type connection, polarization direction in both layers of a bimorph specimen becomes identical whereas, in a series type, polarization direction is opposite. The result is such that the parallel type vibration provides higher amplitude than the series type vis-a-vis the same applied voltage and is used for transmission. On the other hand, the generated voltage becomes larger in a series type connection than the parallel type vis-a-vis the same vibration, and is used at the receiving end.

As shown in Table 2, institutions using parallel type benders at transmitting end and series type benders at the receiving end were the most. By using series type connection in parallel benders and parallel type connection in series benders, all the bender body can be compressed or

Table 2. Test apparatus, test conditions, size and mounting of BE

Lab. No.	Apparatus	Specimen size			Dry			Saturated			Dimension of BE								Material	Electrical connections	
		D (mm)	H (mm)	H/D	$K=1$	$K=0.5$	K_0	$K=1$	$K=0.5$	K_0	L_t (mm)	W (mm)	t (mm) Transmitter	t (mm) Receiver	L_e (mm) Transmitter	L_e (mm) Receiver	t_c (mm)	$2L_e/H$ %		Transmitter	Receiver
1	TX	100	200	2.00	4							10	1.0		2.5			2.5			
2	TX	50	100	2.00				2	2			12	1.5		4.5			9			
3	TX	38	80	2.11	3	3			1		13	12.5	1.6	1.8	3.2	3.6		8.5	PZT		
4	OM	75	40	0.53			2			2	20	10	0.5		3.0			15	PZT		
5	OM(TX)	50	50	1.0			2					12.5	0.51		10			40		Parallel	Series
			90	1.8			3											22.2			
6	TX	66	70	1.06	1						—	10	0.5		5.0		0.5	14.3	PZT	Parallel	Series
7	TX	75	150	2.00				1	2		13	10	0.5		7.0			9.3		Parallel	Series
8	TX	76	150	1.97	3							11	1.2		1.2			1.6			
9	RC/TS	50	100	2.00	2			2			12.7	8	0.6		3.705		0.25	7.4	PZT	Series	Series
10	DS	75	100	1.33			2				13	10	0.5		7.27	6.98		20.4	PZT	Series	Series
11	TX	50	100	2.00				2	2			12	1.2	1.4	4.1	4.4		8.5			
12	RC	50	110	2.20	2	2		3	2		12.7	10	0.5		4.9	3.3		7.5		Parallel	Series
13	TX	70	140	2.00	2	2					20	10	0.5		2.0			2.9	PZT		
14	TX	50	100	2.00				1			12.7	10	0.5		4.575		0.25	9.2			
15	OM	62	55	0.89						2	31.8	12.7	0.38		4.0		0.7	14.5	PZT	Parallel	Parallel
	TX	39	85	2.18				2	2									9.4			
16	TX	50	100	2.00	2	2		2	2		20	5	1.0		8.8	9.4	0.25	18.2	PZT	Parallel	Parallel
17	DS	48	60	1.25			2				15	10	0.5	2.0	10.23	12.63	0.5	47.6	PZT	Parallel	Series
							2				15	10	0.5	2.0	10.23	17.62	0.5	58	PZT	Parallel	Series
							2				15	10	0.5		10.23	12.75	0.5	47.9	PZT	Parallel	Series
							2				15	10	0.5		10.23	17.15	0.5	57	PZT	Parallel	Series
							2				15	10	0.5		10.23	8.45	0.5	38.9	PZT	Parallel	Series
18	TX	70	140	2.00	3						20	10	3.0		2.0			2.9			
19	TX	50	100	2.00				1			12.7	1.65	0.6		1.95			3.9			
20	TX	50	100	2.00	2	1					20	10	0.65		3.0			6	PZT	Parallel	Parallel
21	TX	53	115	2.17	3	2		2	2		12 13	10	0.5		10.5	10.48	0.5	17.9	PZT	Parallel	Series
22	TX	70	70	1.00				2			20	10	0.5		5.93	6.30	0.5	17.5	PZT	Series	Series
			100	1.40				2										12.3			
			150	2.14				2										8.2			
23	TX	200	390	1.95	2			2			12	10	0.5		7.0	5.0	0.5	3.1	PZT	Parallel	Series
					29	12	19	26	15	4											
Total (number of tests)					60			45													
					105																

* Lab. No. does not coincide with Table 1.

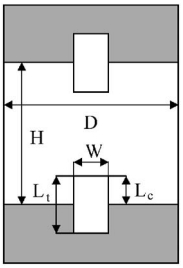

Fig. 2. Dimensions of BE

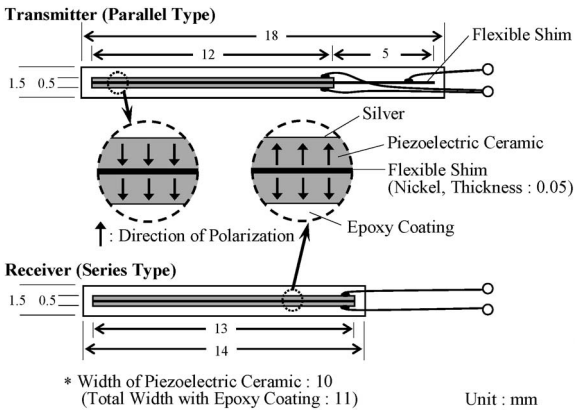

Fig. 3. An example of BE

extended together, thus enabling it to measure P-wave velocity (Lings and Greening, 2001). As discussed later, P-wave velocity was measured by one of the institutions by using this principle.

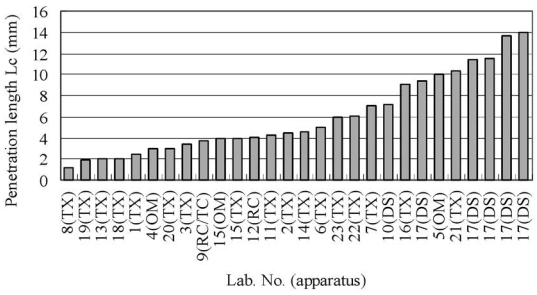

Fig. 4. Penetration length of BE

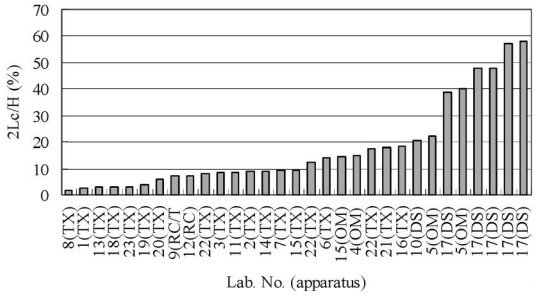

Fig. 5. Penetration length ratio of BE

In order to pass a shear wave into the specimen through the BE and receive it from other end, it is necessary that the BE penetrate into the specimen from either end. There is no clear conclusion about the ideal penetration length. When the penetration is too long, it can disturb the specimen excessively. On the other hand, when it is too short, strength of shear wave may be too weak either in transmission or at reception. In addition, it is possible that NFE is also affected by such changes in penetration length.

Figure 4 shows the average penetration length L_c of benders into the specimen that was used by the participating laboratories (mean penetration length at specimen top and bottom). The length differs largely from institution to institution ranging from 1.2 to 14 mm, with an average of 6.0 mm. On excluding the relatively large penetration from Lab. No. 17, the mean value of penetration comes out to be 4.7 mm. Figure 5 shows the variation of $2L_c/H$, depicting the proportion of penetration as compared to the specimen height H. For the tests conducted, the range varied from 1.6 to 58% with a mean value of 17.5%. The mean value of penetration ratio in triaxial test apparatus and resonance method test comes out to be 8.6%. It became larger and reached 36% in consolidation and shear test equipment whose specimen height is relatively low.

Identification of Travel Time

Table 3 shows the type of input wave and identification method of shear wave arrival time used by different institutions. In the test, shear wave velocity V_S is calculated from the simple measurement of propagation distance Δs and propagation time Δt. It is thus a very simple test.

Regarding the propagation distance, with the exception of two institutions, which designated a distance between the central part of benders and the whole specimen height of sample as Δs, all other 21 institutions considered the tip-to-tip distance between bender pairs as Δs. Thus it is considered that there is consensus on the definition of Δs as the tip-to-tip distance between bender pairs. On the one hand, there was no such international consensus for the identification of arrival time of the received wave. It differed at different tested institutions and is the main issue of discussion in BE test.

Currently, there are three different approaches to identifying the arrival time. The first one is by actually observing the transmission and received wave signal and finding their difference as a propagation time in the soil specimen as shown in Fig. 6(a) (e.g., Dyvik Madshus, 1985; Jovičić et al., 1996). As this method uses a time base axis in order to identify the propagation time, this is often called as time domain technique (T.D.). With this method, when the distance between the bender pairs is short, the received waves are often affected by NFE disturbances that are believed to be the influence of P-wave signals that reach before the actual shear waves. In addition, additional effects by other electric noises and reflections etc., often makes the reading of arrival time quite difficult. To separate the NFE and noise, signal arrival is often observed by passing waves of different frequencies. In addition, measuring the time difference between the first peak of the transmission wave and the corresponding peak of received wave is yet another technique.

The second method is to calculate the cross correlation (C.C.) between transmitted and received wave as shown in Fig. 6(b) (e.g., Mancuso et al., 1989; Viggiani and Atkinson, 1995). This is based on the presumption that the transmitted shear wave retains its wave shape, i.e., frequency, even when it is passed into the soil. In this method, C.C. of transmitted and the received wave is first evaluated and the position at the maximum amplitude is taken as propagation time. However, there are times when frequencies of transmitted and received waves do not agree and the second peak or later at the received wave, rather than the first one, becomes larger in amplitude. In such a condition, there needs an experienced person with a proper knowledge to interpret the correlated result and is a problematic aspect of this testing technique. Furthermore, as this method calculates the arrival time using the time base axis, it is often said to be identical to T.D. The third method calculates the cross spectrum of the transmitting and receiving waves producing the relations of amplitude and phase angle with frequency axis as shown in Fig. 6(c). The arrival time is then calculated from the inclination of phase spectrum. As it uses the frequency characteristics of input and output waves, it is often called as frequency domain technique (F.D.) (e.g., Blewett et al., 1999; Greening and Nash, 2004).

During the early days when BE was used, shear wave velocity was calculated based on the travel time of a square wave signal and considering the time to the first

Table 3. Input wave and identification method of travel time

Lab. No.	Apparatus	Wave shape	Input V ± V	Frequency kHz	Identification of Travel Time			Δs	Data time Inter. μs
					T.D.	C.C.	F.D.		
1	TX	sin pulse	5	5–10	S-S			tip-to-tip	10
		rect. pulse	5	5–10					
2	TX	rect. pulse	15–25	5(10)	S-S			mid.-to-mid.	0.1–0.5
3	TX	sin pulse	10	4–10		○	unit-inpuls response frequency response	tip-to-tip	—
4	OM	sin pulse	10	15(20, 30)	P-P			tip-to-tip	1–10
5	OM(TX)	sin pulse	10	15	plural points with S-S	○		tip-to-tip	10
		sin sweep	10	1.5–20			ABETS		
6	TX	rect. pulse	10	—	S-S			tip-to-tip	12
7	TX	sin pulse	20	4	S-S			tip-to-tip	2
8	TX	sin pulse	5	10		○		tip-to-tip	10
9	RC/TS	sin pulse	10	11–15	S-S			tip-to-tip	0.5
		rect. pulse	10	0.6–15					
10	DS	rect. pulse	10	0.027	P-P			tip-to-tip	0.25
11	TX	sin pulse	10–30	5–15	S-S	○		tip-to-tip	2
12	RC	sin pulse	10	15	?			tip-to-tip	—
13	TX	sin pulse	10	10–20	S-S			tip-to-tip	2
14	TX	sin pulse	10	15	?			base-to-base	—
15	OM	sin pulse	10	55(60)	S-S			tip-to-tip	0.04
	TX	sin pulse	10	10(−20)					0.1–0.2
16	TX	sin pulse	10	1.5(−10)	S-S			tip-to-tip	1–5
17	DS	sin pulse rect. pulse	10	0.1–10	plural points with S-S			tip-to-tip	2.5
18	TX	sin pulse	10	2–8	S-S			tip-to-tip	0.4–12
		sin cont.	10	5–27			π-point (Lissajous)		
		sin sweep	10	5–19			ABETS		
19	TX	sin pulse	—	—	S-S			tip-to-tip	0.4
20	TX	sin pulse	10	2.7–33	plural points with S-S			tip-to-tip	1
		rect. pulse	10	0.005					
21	TX	sin pulse	20	5–20	S-S			tip-to-tip	0.1
		rect. pulse	20	0.1					
22	TX	sin pulse	10–50	5–20	S-S			tip-to-tip	0.5–1
23	TX	PRBS	25	4		○		tip-to-tip	15

peak of the received wave as a propagation time (e.g., Dyvik and Madshus, 1985). But, considering the fact that a square wave is simply a summation of number of sine waves of various frequencies, it was considered to use sine wave input that has a single frequency. Because of the difficulty in identifying the arrival time due to the influence of aforementioned NFE, C.C. method was proposed as a better alternative by some researchers (e.g., Viggiani and Atkinson, 1995). Identification of signal arrivals with frequency domains is discussed in Greening and Nash (2004).

As shown in Table 3, regarding the identification method used in defining propagation time for this study, there are laboratories which used multiple methods but T.D. technique was most commonly used. Regarding the input wave shape in T.D. method, 10 laboratories used only the sine wave, 3 laboratories used only the rectangular wave and 5 laboratories used both types. Thus 15 out of 18 laboratories were using sine wave input for their study.

For C.C. method, the use of sine wave input is universal because of the need to calculate C.C. function of the transmitted and the received waves. A laboratory employed PRBS (Pseudo Random Binary Sequence) wave. In the case of F.D. method, in order to obtain the frequency characteristic of the transmitted and received wave, either the sweep or the continuous signal of sine wave was applied. Besides, there were two institutes which did not report identification method.

Regarding the voltage for the input signal, the institutes which used ±10 V were the most. A few of the laboratories used voltage amplifier to magnify the input voltage and it was as high as ±50 V at the maximum. Relating the frequency for the test cases using sinusoidal input wave and considering T.D. method, 5 institutes used single frequency input wave under the same consolidation conditions but 9 others varied the input frequency.

Regarding the identification method of propagation time on T.D. method of defining arrival time, the time difference between the starting point of the transmitted wave and the corresponding point in received wave (start-to-start: S-S) has been considered as the propagation time

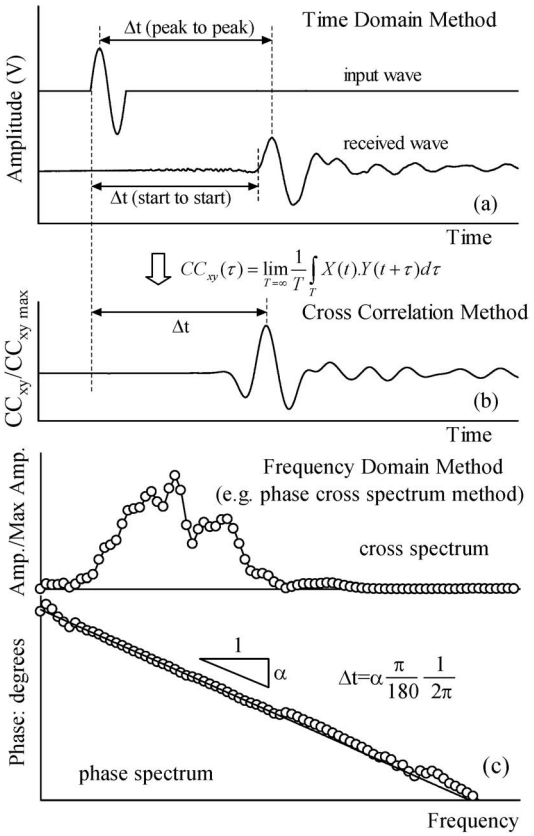

Fig. 6. Typical identification methods of travel time; (a) time domain method, (b) cross correlation method and (c) frequency domain method

by 13 institutes whereas, the time difference between the peak point of the transmission wave and the corresponding peak in the received wave (peak-to-peak: P-P) is considered by two institutes. Besides, there were records by three other institutes which observed the definition of arrival time by considering different points in the received wave.

It is to be noted that the accurate arrival point is not understood correctly from the received wave if the sampling interval is too large. Table 3 also shows the sampling interval of the wave data reported by different institutes. For example, in the case of dry sand having propagation velocity V_S of 250 m/s (80% relative density, i.e., $\rho_d=1.553$ g/cm^3 and $G=97$ MPa) and propagation distance Δs of 100 mm, propagation time $\Delta t=0.1/250$ sec $=400\,\mu$s. To read the arrival time in the order of 1% accuracy, the sampling interval should be at least 4 μs as shown in Fig. 7. When the frequency of received portion of wave becomes as high as 10 kHz, as an example, reading 100 points per wave needs the accuracy of 1 μs. Although actual sampling interval also depends upon the travel distance of shear wave signal, it is expected that the interval lies within a few micro seconds. Among the intervals shown in Table 3 and Fig. 7, there are cases which used 10 μs or more time interval. There is a need for the participated laboratories to increase the sampling speed, in order to increase the precision in identifying the true received signal.

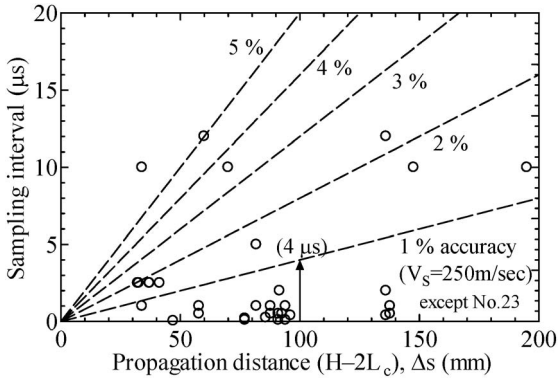

Fig. 7. Effect of sampling interval on accuracy of arrival time

In this way, although various methods were adopted for the identification of propagation time by different institutions, time difference between the start of the transmitted and received waves (start-to-start, S-S) was mostly used by using single cycle of sinusoidal wave and considering the influence of NFE by passing waves of different frequencies.

TEST RESULTS

Relations between G and e

Figures 8 to 10 show the relation between shear modulus G and void ratio e for isotropically consolidated specimens ($K=\sigma'_h/\sigma'_v=1.0$), anisotropically consolidated specimen with $K=0.5$ and K_0-consolidated specimen at the vertical stress σ'_v of 200 kPa. In the figures, results of saturated specimens as well as dry specimens are shown collectively. A solid line in each plot shows the relationship of $G=14100f(e)\sigma'^{0.4}_v$ (kPa) ($G=900f(e)\sigma'^{0.4}_v$ (kgf/cm^2)) at the shearing strain of 10^{-6} and at different confinements, where $f(e)=(2.17-e)^2/(1+e)$, (Iwasaki and Tatsuoka, 1977). The relation was obtained from the test performed in a resonant column apparatus by using a clean sand of very small U_C, similar to the Toyoura sand.

The result (Fig. 8) for the specimen at isotropic consolidation ($K=1.0$) shows that an increase in isotropic stress narrows down the amount of scatter in the data. Furthermore, the scatter in test data is larger for dry specimens than the saturated ones. Figure 9, showing the plot for anisotropically consolidated ($K=0.5$) specimen, also shows the very similar trend of the decrease in scatter at higher stress and when saturated as discussed above for an isotropic case. On the other hand, Fig. 10 that plots the results for K_0-consolidated specimens shows a very large variation in the value of G for dry specimens.

The above discussion, based on the plots of entire data, shows that data scatter varies depending upon the test condition, especially, when the specimen is dry and for K_0 -consolidated specimens that are performed in a stiff metal containers and comparatively smaller travel length. The following could be some of the several reasons for these variations.

As explained previously, the arrival time identification method differed at each of the laboratories who per-

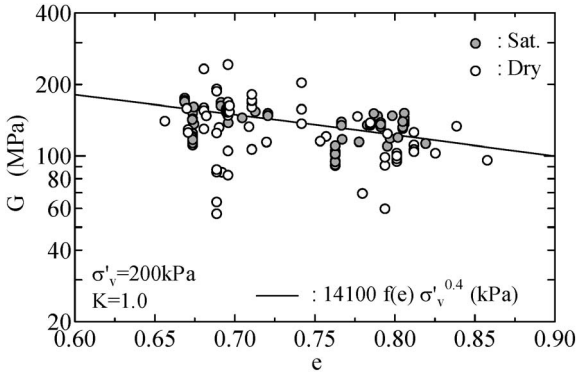

Fig. 8. Relations of G and e ($K=1.0$, $\sigma'_v=200$ kPa)

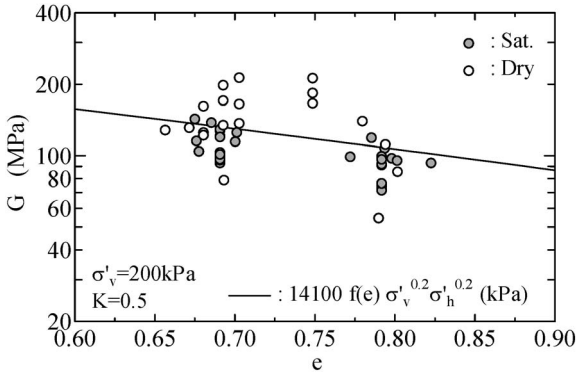

Fig. 9. Relations of G and e ($K=0.5$, $\sigma'_v=200$ kPa)

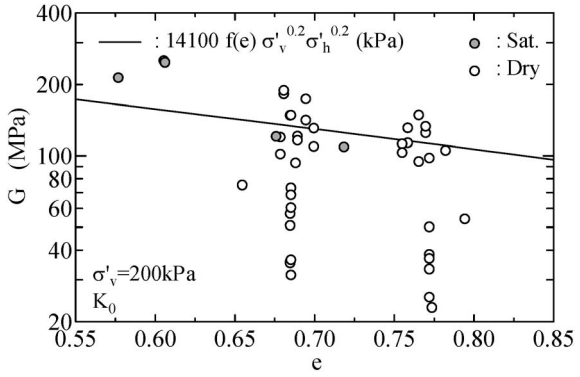

Fig. 10. Relations of G and e (K_0, $\sigma'_v=200$ kPa)

formed the tests. For example, in a T.D. method that measures the arrival position of the shear wave from the received signal, various groups assumed different points in the received wave as the true arrival position and calculated the G values accordingly. In this way, calculated G value was different even for the identical specimens prepared in the same laboratory. In addition, one can expect very large effect of time definition in the result of G value when the travel path through the soil specimen is smaller, such as for K_0-consolidation tests and direct shear apparatus. Moreover, since the effects of NFE are larger in dry specimens as mentioned earlier, it is considered that the scatter was more significant for the dry specimens

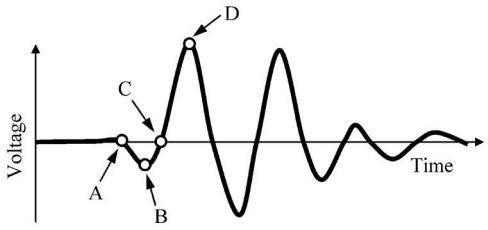

Fig. 11. An example of arrival point

than the saturated ones. Furthermore, even when the S-S definition has been considered as the arrival time, the exact location considered for the wave arrival in a received wave differed among the testing group. When asked with an example of received wave, such as in Fig. 11, the reading point varied from A, B, and C depending upon the participating teams.

In such circumstances, it can be well envisaged that the scatter, such as observed in Figs. 8 to 10, is not actually the real scatter of the BE test. In order to show the actual waveform variation, the data from laboratories, which performed the experiments by using single pulse sine wave as an input and have submitted time history of both input and received waves, are extracted below for an illustration.

Wave Data

Figure 12 shows the examples of the received waveform obtained from the single cycle sine or rectangular waves input for isotropically consolidated specimens at the confinement of 200 kPa. In this figure, the time based lateral axis of the wave has been normalized with the respective tip-to-tip distance of benders for comparison. The horizontal axis thus becomes the inverse of shear wave velocity. The received waveforms are representative samples of different participating teams. The vertical arrow sign (↓) in the wave indicates the point which was considered as the shear wave arrival time by them. It can be noticed that the arrival point falls inside a relatively narrow band, excluding the result from Lab. No. 16. The reason for such a large difference in the result of Lab. 16 could be due to relatively smaller frequency of 1.5 kHz and low resolution of measuring equipment used in data reception.

Figure 13 shows the same data as plotted in Fig. 12. In the plots, the horizontal axis in Fig. 12 is further normalized with a parameter $(\rho_t/f(e))^{0.5}$, where ρ_t = wet density, $f(e)=(2.17-e)^2/(1+e)$. In other words, the inverse of the square of the function plotted in horizontal axis takes the form of $G/f(e)$ (kPa). As shown in Figs. 12 and 13, the void ratio of the prepared samples differs among different laboratories. It is therefore, considered that introduction of void ratio function would eliminate the error introduced by the void ratio difference. Comparatively narrower scatter band width Fig. 13 confirms this assumption. This means that if the wave reading is taken by following S-S method, the accuracy within the band width is ascertained. If converted into $G/f(e)$ value, the expected ranges are from about 90 to 130 MPa.

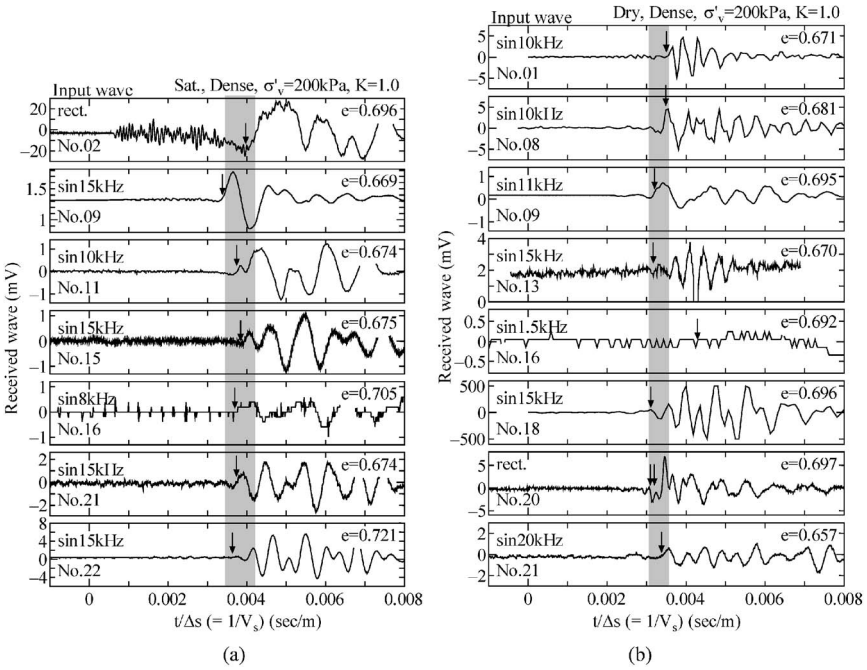

Fig. 12. Examples of wave data ($K = 1.0$, $\sigma'_v = 200$ kPa, $D_r = 80\%$); (a) saturated specimen and (b) dry specimen

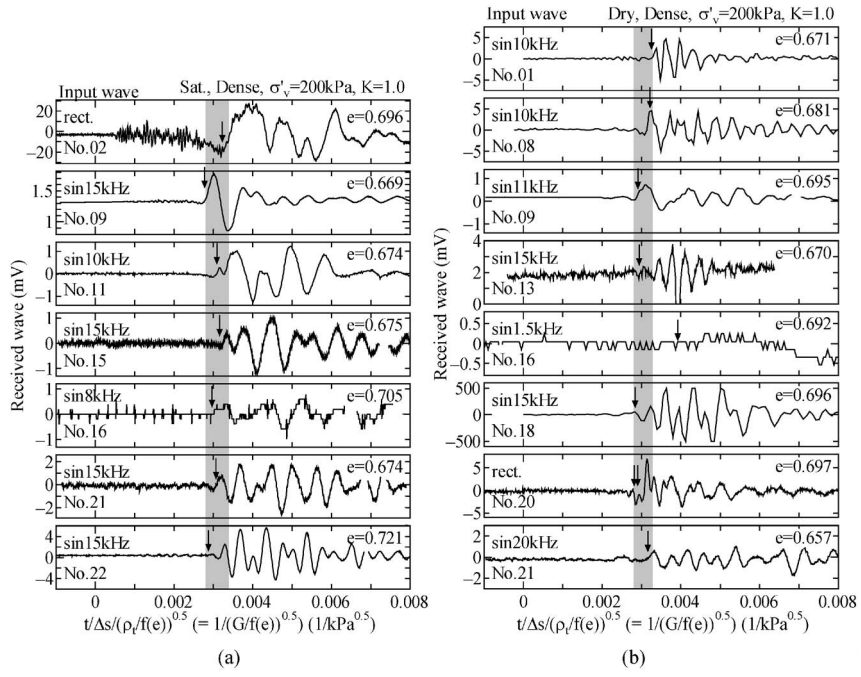

Fig. 13. Examples of normalized wave data ($K = 1.0$, $\sigma'_v = 200$ kPa, $D_r = 80\%$); (a) saturated specimen and (b) dry specimen

In summing up the above discussions, if the S-S method is considered for arrival time definition, the accuracy in getting G by using BE test falls in a narrow range, indifferent of whether the tests are performed in dry or saturated condition.

Effect of Arrival Time Identification Method

If the data reported from all the laboratories were plotted, a large variation in G value was noticed as discussed above. The following reasons are believed to be the main factors for such variations:

i) Method of arrival time identification differed with each laboratory.
ii) Even for the same identification method, reading points differed with laboratory.
iii) Some laboratories even considered multiple points in the received wave as arrival time and calculated multiple values of G.

On the other hand, when the actual received wave was compared as discussed in the above section, large varia-

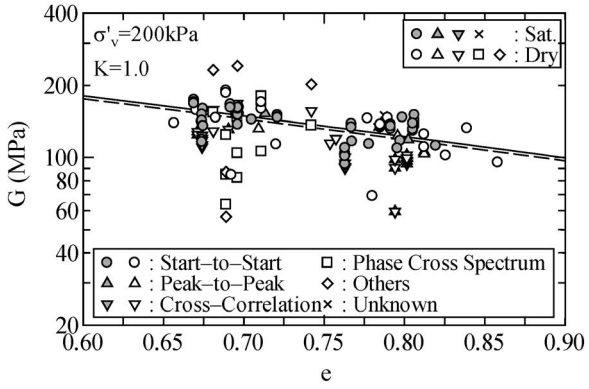

Fig. 14. Effect of identification method of travel time ($K=1.0$, $\sigma'_v=200$ kPa)

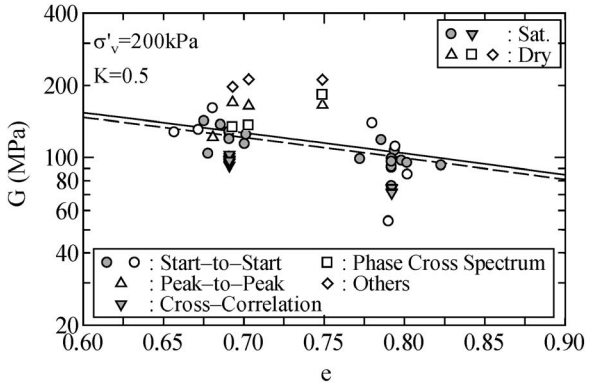

Fig. 15. Effect of identification method of travel time ($K=0.5$, $\sigma'_v=200$ kPa)

tions did not exist. Therefore, comparison of the test results was done as hereunder, based on the difference in the arrival time identification method.

Figure 14 plots the relationship of G vs. e at 200 kPa for isotropically consolidated specimens by using the data submitted from testing laboratories. The solid line in the figure shows the relationship of $G=14100f(e)\sigma'^{0.4}_v$ (kPa) ($G=900f(e)\sigma'^{0.4}_v$ (kgf/cm^2)) (at $\gamma=10^{-6}$) and the dashed line, $G=11100f(e)\sigma'^{0.44}_v$ (kPa) ($G=850f(e)\sigma'^{0.44}_v$ (kgf/cm^2)) (at $\gamma=10^{-5}$) (Iwasaki and Tatsuoka, 1977). The following points are noted from these figures:

i) S-S method of identification results in a relatively smaller variation as compared with other methods. The data points also match well with the relations obtained independently in the past researches.
ii) P-P and C.C. methods yield slightly smaller values of G as compared with S-S method.
iii) It seems that G values are not affected by the saturation condition but larger scatter were found in the results for dry specimens.

Figures 15 and 16 plot the G vs. e relationship reported from different laboratories for anisotropically consolidated samples at $K=0.5$ and K_0-consolidated samples performed in stiff metal containers when vertical stress was 200 kPa. The following trends of behaviour are observed from these figures:

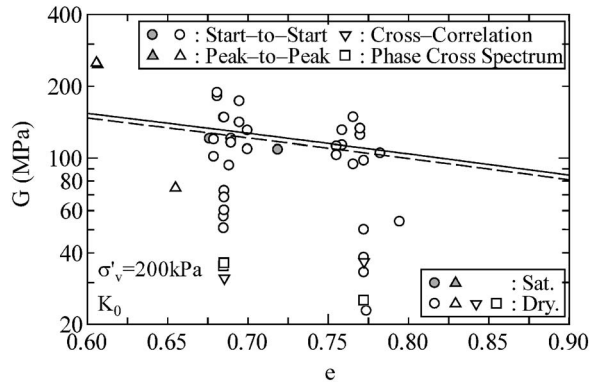

Fig. 16. Effect of identification method of travel time (K_0, $\sigma'_v=200$ kPa)

i) G values obtained from K_0-tests, where specimens were put inside a stiff metal container, are relatively smaller and have large scatter than other results.
ii) Results from anisotropically consolidated tests ($K=0.5$ and K_0) are relatively largely scattered as compared with isotropically consolidated tests.
iii) Very similar to the isotropic specimens, G values from anisotropic tests calculated by defining the arrival time with S-S method has comparatively smaller scatter. Besides, the data points are very close to the solid lines shown in the figure.

RE-EVALUATION OF TEST DATA

As expressed in the description above, scatter results due to the difference in identification method and also because the actual reading point differs according to the personal judgment when T.D. method is applied. Therefore, it is neither convincing nor appropriate to evaluate the BE test method from only the reported test data. At this point, the whole wave data was reread by applying the single identification method from the digital records of the waveforms provided by testing laboratories.

Used Identification Methods

Start-to-Start Method

From among the digital waveform data received, laboratories which used single pulse of sine or square wave as an input were reread by using S-S method of the arrival time definition. The NFE and direction of the initial motion of BE against the applied voltage was considered while deciding arrival point in the received signal.

There were very few laboratories which provided the information of the initial movement of benders on applying electric voltage. In this regard, it was presumed that the initial motion of BE for both transmitting and receiving side fell on the same side if such information was not supplied.

To consider NFE, receiving signals obtained by exciting the transmitter bender with sinusoidal waves of different frequencies, needs to be compared and evaluated (if available). When the first amplitude in reception time

history matches the direction of initial motion, the point where the receiving signal takes-off from the zero line (a horizontal line of voltage output when there is no signal) is the time of shear wave arrival. In this case if the first amplitude in reception time history does not match the direction of initial motion, the point on the wave when it first traverses to the direction of initial motion and intersects the no-signal line is the arrival time of shear waves as shown in Fig. 17 (e.g., Kawaguchi et al., 2001).

Peak-to-Peak Method

Similar to the S-S method above, the data from laboratories that used single pulse of sine wave input were reread by using P-P method, i.e., the time lag in between the peak position of an input wave to the first peak of the received wave, as the definition for arrival time. At the time of identification, direction of the initial motion of BE was considered similarly as that for S-S method described earlier.

Cross Correlation Method

The shear wave arrival time was also re-evaluated from C.C. technique by using Eq. (1) after selecting only those data from the whole pool which used single sine wave pulse as an input. If the first received signal has the biggest amplitude, the arrival time was defined at the position where the highest peak of correlation was located. However, when the first peak at reception was not the highest one, the first peak in the time history of C.C., rather than at highest amplitude, was taken as the required arrival time. Besides, the direction of the initial motion of BE was considered similarly as described earlier.

$$CC_{xy}(\tau) = \lim_{T=\infty} \frac{1}{T} \int_{T} X(t) \cdot Y(t+\tau) d\tau \qquad (1)$$

Here, $CC_{xy}(\tau)$: cross correlation function, T: recording period, $X(t)$: time history of input wave, $Y(t)$: time history of received wave, τ: delay.

Phase Cross Spectrum Method

The cross spectrum and its associated phase angle is obtained by performing Fourier transformation of C.C. function. The average inclination of absolute phase angle at the cross spectrum, if evaluated at the prevalent frequency of match between input and received waves, phase velocity of shear wave propagation time can be obtained. For the details on this method, please refer Viggiani and Atkinson (1995). If this inclination is designated as α, shear wave propagation time, Δt is given by the following formula.

$$\Delta t = \alpha / 360 \qquad (2)$$

Re-evaluation by Start-to-Start Method

In Figs. 18 to 23, the horizontal time axis of the reported wave data has been normalized with the distance between tip-to-tip of bender pairs and further normalized with the square root of the ratio of the wet density and a void ratio function $f(e)$. The zero in the figure denotes the start of input wave and the ordinate is simply the amplitude of the received voltage. These 6 figures are prepared based on dry and saturation conditions and testing methods for specimen at $D_r = 80\%$. The number at the bottom left of the figure is the laboratory number and the vertical line corresponds to the defined arrival point.

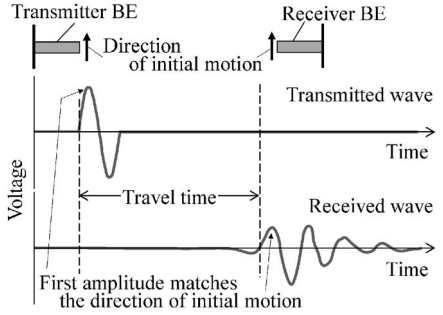

Fig. 17. Used identification method by the start-to-start technique

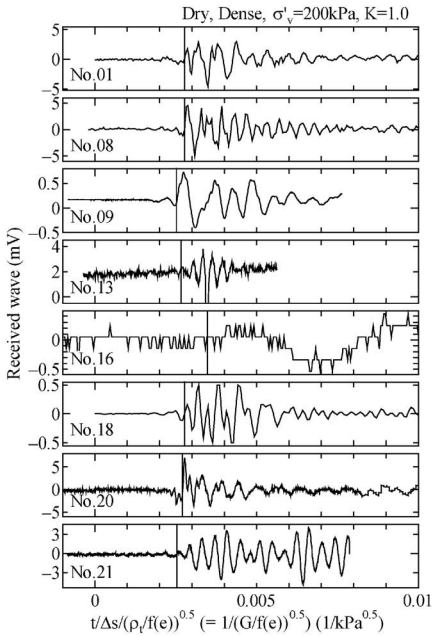

Fig. 18. Wave form on start-to-start method (dry specimen, $K = 1.0$, $\sigma'_v = 200$ kPa, $D_r = 80\%$)

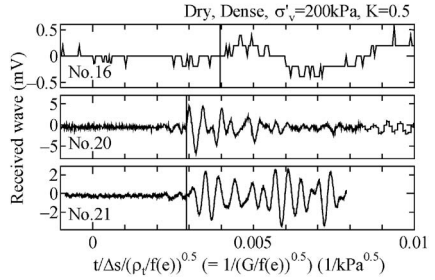

Fig. 19. Wave form on start-to-start method (dry specimen, $K = 0.5$, $\sigma'_v = 200$ kPa, $D_r = 80\%$)

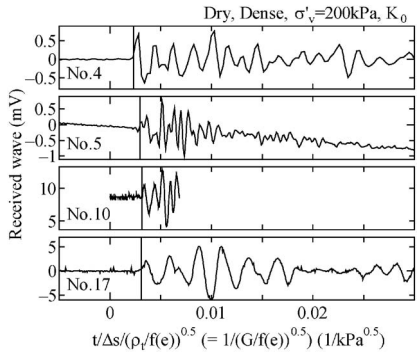

Fig. 20. Wave form on start-to-start method (dry specimen, K_0, σ'_v = 200 kPa, D_r = 80%)

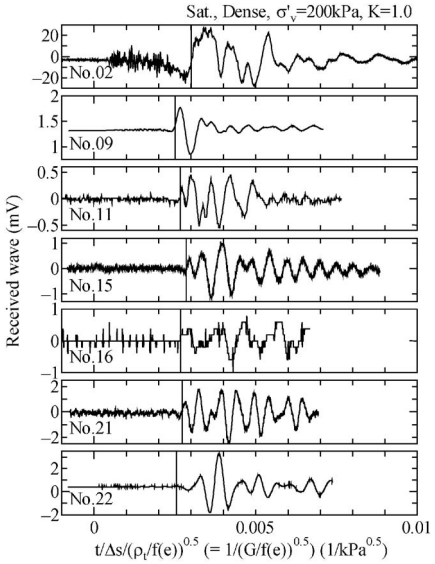

Fig. 21. Wave form on start-to-start method (saturated specimen, K = 1.0, σ'_v = 200 kPa, D_r = 80%)

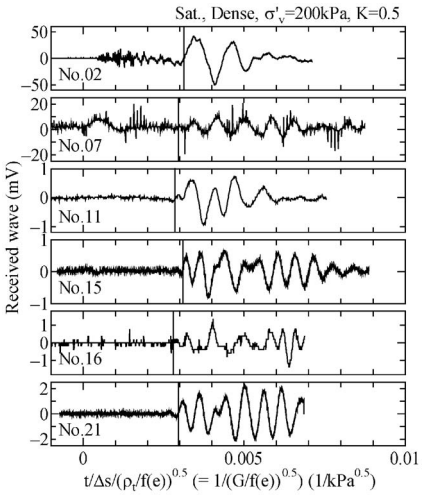

Fig. 22. Wave form on start-to-start method (saturated specimen, K = 0.5, σ'_v = 200 kPa, D_r = 80%)

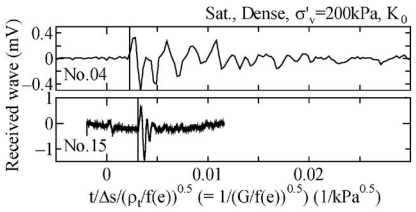

Fig. 23. Wave form on start-to-start method (saturated specimen, K_0, σ'_v = 200 kPa, D_r = 80%)

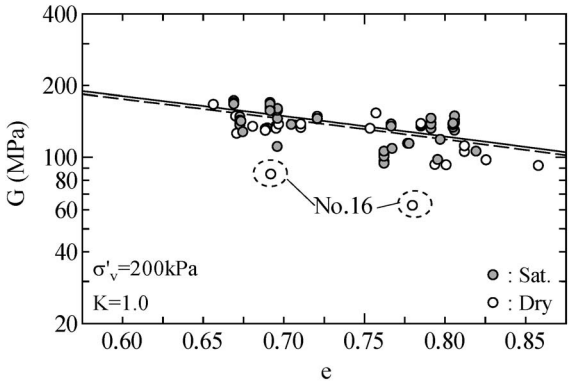

Fig. 24. Re-evaluation results on start to start method (K = 1.0, σ'_v = 200 kPa)

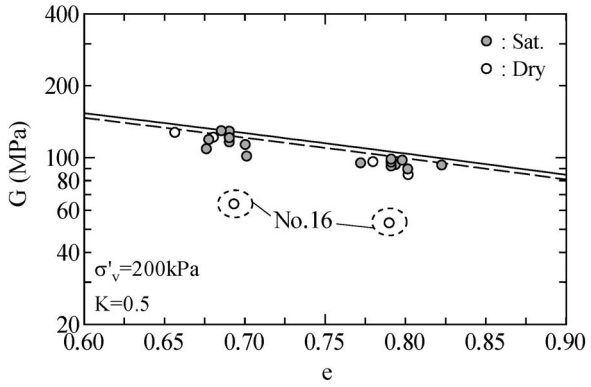

Fig. 25. Re-evaluation results on start to start method (K = 0.5, σ'_v = 200 kPa)

While plotting the figure, if only one signal record was found, the same was plotted irrespective of the input wave frequency. However, if there was data of more than single frequency, wave data in the range of 10–15 kHz was selected for plotting.

Figures 24 to 26, respectively representing K = 1.0, K = 0.5 and K_0-tests, compare the G values that were evaluated by a standard technique of the S-S method. Although a little variation in the G value still remained, the scatter remarkably narrowed down if compared with the original submissions from the laboratories. Encircled data points in Figs. 24 and 25, which are located away from other data, are from the Lab. No. 16. It is considered that such scatter is not only due to the relatively long sampling interval of received wave, but also because of a very low

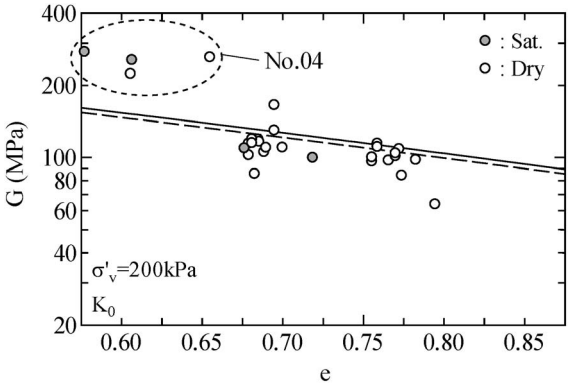

Fig. 26. Re-evaluation results on start to start method (K_0, $\sigma'_v = 200$ kPa)

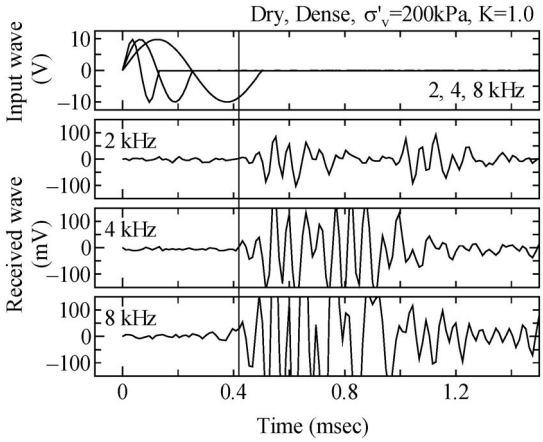

Fig. 27. Effect of frequency ($K = 1.0$, $\sigma'_v = 200$ kPa, $D_r = 80\%$, Dry, Lab. 18)

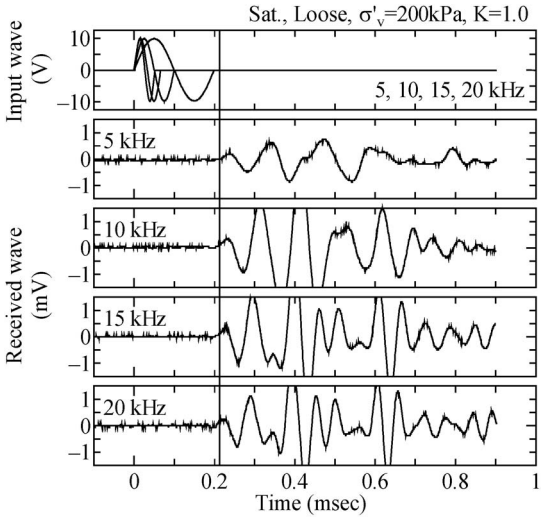

Fig. 28. Effect of frequency ($K = 1.0$, $\sigma'_v = 200$ kPa, $D_r = 50\%$, Saturated, Lab. 22)

frequency of the input sine wave (1.5 kHz). For example, in Fig. 21 for a saturated specimen, the result submitted from the same laboratory but at higher frequency of 6 kHz resulted in the G values in par with other laboratories. Therefore, when receiving voltage is small and the resolution is rough, it is difficult to pinpoint the arrival point accurately. For clear reception, it is either necessary to increase the data resolution or to enlarge the received signal by increasing transmission voltage or input wave frequency. In Fig. 26, encircled data points of Lab. No. 4 are also located away from other data. The average void ratio of No. 4 is about 0.6, i.e., the relative density is over 100%. It may have been that the vertical stress was applied in considerable excess. Excluding the data from Lab. Nos. 4 and 16, the re-evaluated results exhibited a far smaller scatter than the original data submitted by the laboratories.

If wave arrival point is properly reread, even the data from Lab. No. 5, which locates quite away from the other data points in Fig. 16, comes closer as shown in Fig. 26. An example of the time history of receiving wave from the Lab. No. 5 is shown in Fig. 20. The wave record is not much different from other submissions. The scatter probably appeared due to the judgment of person in charge of interpretation. It is most likely that the initial shear wave signals which are quite weak are considered as a noise while judging the arrival point. The larger value of travel period considered at the highest amplitude points might have resulted into extremely low G values. In this way, although some experience is necessary, sufficiently reasonable values of G can be obtained, if the S-S method of wave arrival technique is applied and NFE is properly considered by paying attention to the direction of initial motion of BE, and wave patterns at different frequencies.

Figures 27 and 28 compare the waveform data received from the same laboratory when the input frequency was altered. The vertical line in each figure shows the arrival time identified by the S-S technique. The following conclusions may be drawn from these figures:

i) In case of dry samples, where frequencies of transmitted wave and receiving wave differ remarkably, the P-P identification method is quite difficult.

ii) Changing the input frequency does not alter the frequency of the received wave appreciably (rather, the receiving wave is thought to be dictated by the test equipment system).

iii) At higher frequencies, such as with $D_r = 80\%$ (Fig. 27), amplitude of received voltage before the initial motion of benders becomes large.

Figure 29 shows the relationship between transmission frequency and shear modulus G. Here, $G_{corrected}$ in vertical axis is corrected for void ratio difference, i.e., current void ratio of the specimen and void ratio corresponding to $D_r = 50$ or 80%, by using void ratio function $f(e)$. There is no clear effect of input frequency in case of the saturated samples but for dry specimens it seems that scatter is slightly on the higher side at lower frequencies. In this figure, data points connected with lines are from the same laboratory performed with multiple input frequencies. In this way, it seems that the value of G increases upon the increase of frequency but the influence is comparatively smaller than other factors.

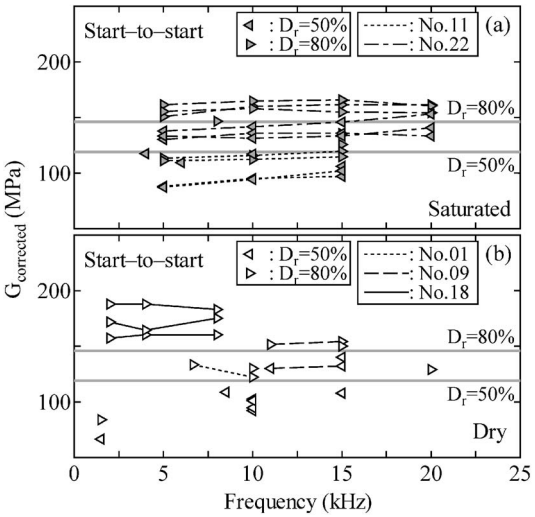

Fig. 29. Effect of frequency ($K=1.0$, $\sigma'_v=200$ kPa); (a) saturated and (b) dry

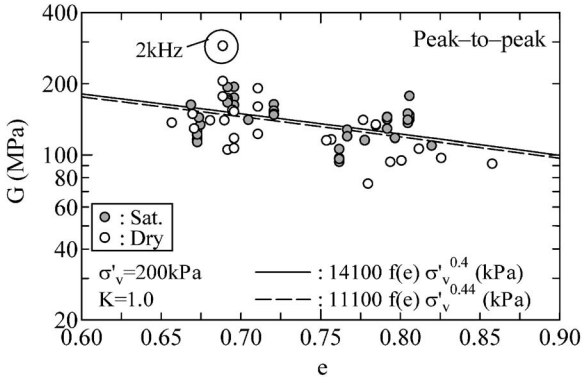

Fig. 30. Re-evaluation results on peak to peak method ($K=1.0$, $\sigma'_v=200$ kPa)

Re-evaluation by Peak-to-Peak Method

Figure 30 plots the re-evaluated G values vs. void ratio e when single sine wave pulse was used as input and arrival time was identified by the P-P method, i.e., the time lag between the peak points of transmitting and receiving waves. Although some scatter in data for dry specimen remained, the re-evaluated results had far smaller scatter than the original data supplied by laboratories. An encircled data point in the figure, which lies away from other points, was obtained by an input of very small frequency of 2 kHz as compared with the input frequency used by other laboratories. As shown with examples in Figs. 27 and 28, the frequency of receiving wave does not change in the same proportion with input frequency. It is due to this reason that the chances of error in arrival time reading go up when the frequency difference between the input and receiving wave goes on increasing.

Re-evaluation by Cross-Correlation Method

Figure 31 shows G vs. e plot for isotropically consolidated specimens at 200 kPa, by identifying the shear wave arrival time with the C.C. method. The data was

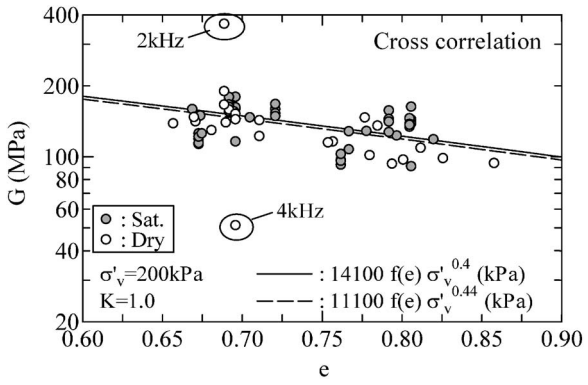

Fig. 31. Re-evaluation results on cross correlation method ($K=1.0$, $\sigma'_v=200$ kPa)

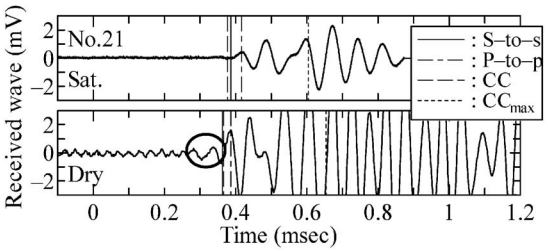

Fig. 32. Comparison of saturated and dry specimens ($K=1.0$, $\sigma'_v=200$ kPa, Lab. 21)

however, limited to the cases where single pulse sine wave transmissions were adopted. As mentioned above, if the first received signal had the biggest amplitude, the arrival time was defined at the position where the highest peak of correlation was obtained. However, when the first peak at reception was not the highest one, the first ever peak in the time history of C.C., rather than at highest amplitude (CC_{max}), was taken as the required arrival time.

As shown in the figure, the time corresponding to the cross-correlated data also has smaller scatter as observed in reread figures explained earlier. On the other hand, the encircled data in the figure representing dry specimens differ quite a lot. It is to be noted that the input frequency for these cases were quite low. As expressed earlier in the P-P method, the frequency of receiving wave does not always increase proportionately according to an input frequency. The error magnitude for the C.C. method, which assumes the frequency similarity of input and received waves, is likely to increase when the frequency difference between them goes up, very similarly to the P-P method.

Observing as a whole, the scatter in the dry specimen is higher than in the saturated ones in the same way as has occurred in previous cases. Figure 32 provides a comparative view of the waveform in saturated and dry sample that were submitted from the same laboratory. From this figure, it is well noted that the amplitude of the received wave for dry specimens is larger, it has longer reverberation time (after effect continues for a long period), and there is bigger noise before the real shear wave signal than saturated cases. It is thought that the

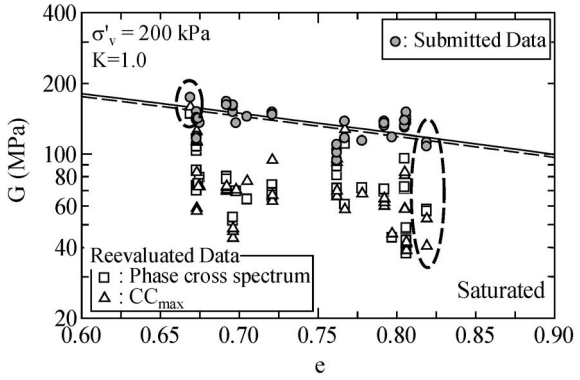

Fig. 33. Re-evaluation results on phase cross spectrum method ($K=1.0$, $\sigma'_v=200$ kPa, saturated specimen)

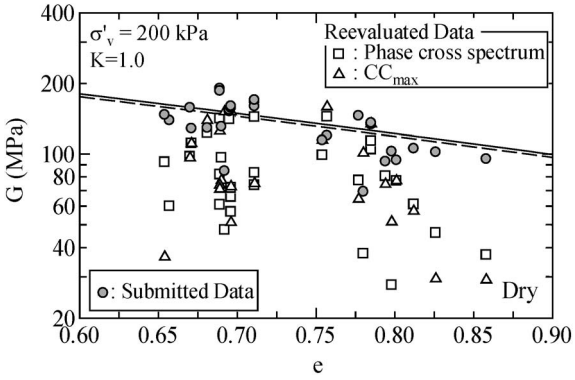

Fig. 34. Re-evaluation results on phase cross spectrum method ($K=1.0$, $\sigma'_v=200$ kPa, dry specimen)

aforementioned effects associated with dry specimens, that create more disturbances in the wave shape, might be the reason behind the larger scatter in dry specimens. Furthermore, the arrival time evaluated by C.C. method is almost identical to that identified by other methods shown in the same figure. In the figure, a little rightward shift in the P-P identification method is not the real difference but because the zero point in the figure is the starting point of input wave, rather than the peak position needed for this method. In addition, CC_{max} that locates the maximum amplitude point in C.C. function, differs more largely than the other result. This clearly tells that when largest amplitude of the receiving wave is not the first wave, there is a high chance of having a big error by adopting CC_{max} method of definition.

Re-evaluation by Phase Cross Spectrum Method

Figure 33 has been prepared for shear modulus G by applying the arrival time identification method of the phase cross spectrum for isotropically consolidated saturated specimens at confinement of 200 kPa. Similar to the P-P and C.C. method, the wave data that used sine wave input was selected from among the whole list of submitted data.

In the figure, the values of G submitted by the laboratories are represented by circular symbol. Coincidentally, all of the laboratories selected here used the S-S method of identification. Plotted in the same figure are the G values corresponding to the time defined by CC_{max} and two general relations obtained for the similar material in the past (solid and broken lines).

The results from some laboratories are almost identical irrespective of the evaluation method (broken circle on the left). But most of the G values obtained from the phase cross spectrum are considerably smaller than those evaluated by the S-S method and are quite scattered (*see* a typical example, the broken circle in the right). On the one hand, G values which are obtained from the phase cross spectrum are almost identical to the G values obtained from the maximum of C.C. function, CC_{max}.

Figure 34 is prepared very similarly to Fig. 33 but for the case of dry specimens. Similar to the saturated specimens, G values for dry specimens are remarkably smaller

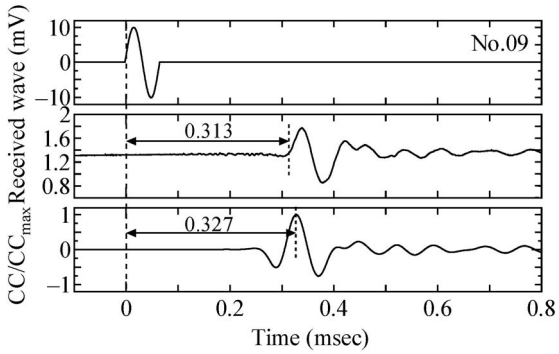

Fig. 35. An example of CC ($K=1.0$, $\sigma'_v=200$ kPa, saturated specimen, Lab. 9)

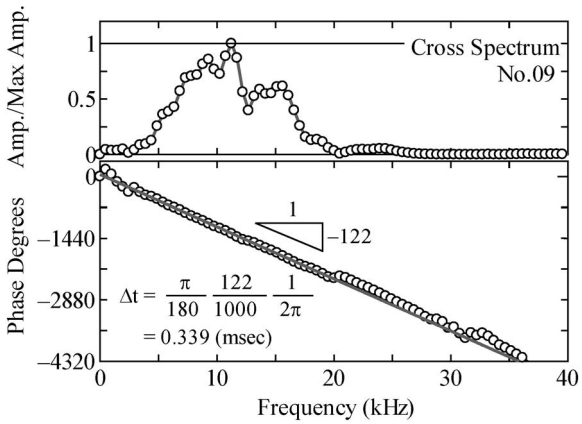

Fig. 36. An example of PCS ($K=1.0$, $\sigma'_v=200$ kPa, saturated specimen, Lab. 9)

than those evaluated by S-S method and are quite scattered. Here, the G values obtained from the phase cross spectrum also differ from the G values obtained from CC_{max} method.

Figures 35 and 36 show the waveform data where the same G value was obtained by any method. If the receiving wave is examined (the second tier), the amplitude of the first signal is the largest. It is expected that this peak point in the receiving wave is considered while calculating

the C.C. function at the maximum amplitude (CC_{max}). As a result, the arrival time calculated from the inclination of phase spectrum in the frequency range where amplitude of the cross spectrum is large (5–20 kHz), is almost equal to the arrival time defined by S-S method.

Figures 37 and 38 compare the arrival time defined by S-S method and by the phase cross spectrum. Unlike in Figs. 35 and 36, the results obtained from different methods differ largely. Looking at the receiving wave (the second tier), the amplitude of the first peak of shear wave is not the largest. The maximum of C.C. function shown in the same figure (the third tier) clearly shows that CC_{max} does not correspond to this first peak. As a result, although the arrival time obtained from the maximum of C.C. function and inclination of the phase cross spectrum (10 to 20 kHz) match fairly, these differ largely with the arrival time determined by S-S method.

Recollecting the above discussions, if the value which is obtained from S-S method or the relational expression of G is taken as the appropriate arrival time, the value of G obtained from the time corresponding to the inclination of the phase cross spectrum will be appropriate only when frequency of input wave is made equal to the frequency of the first wave appeared in receiving wave.

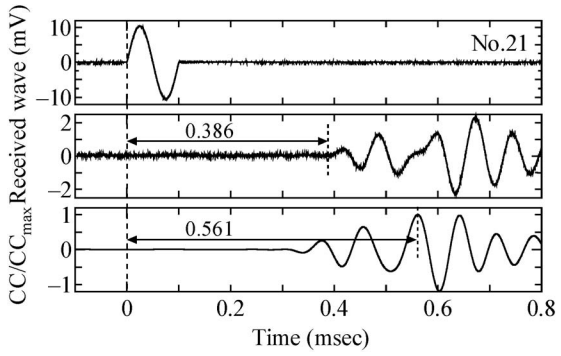

Fig. 37. An example of CC ($K=1.0$, $\sigma_v'=200$ kPa, saturated specimen, Lab. 21)

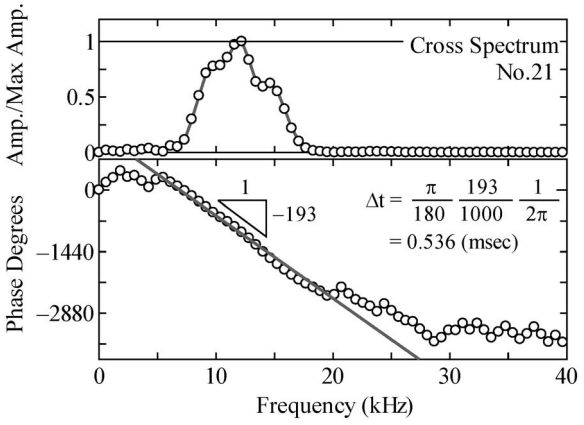

Fig. 38. An example of PCS ($K=1.0$, $\sigma_v'=200$ kPa, saturated specimen, Lab. 21)

COMPARISON WITH OTHER TESTS RESULTS

In the current series of parallel test, besides finding shear wave velocity using the BE, it was also requested to find elastic moduli from the stress-strain curve by applying either monotonic or cyclic loads with strains 0.001% or less. Table 4 shows test condition and testing methods other than BE testing applied to determine the Young's modulus E and shear modulus G.

Among the laboratories which submitted reports, 12 out of 23 provided results obtained from other than BE method. Within those 12, nine of them obtained E values by using cyclic loads at very small strains (CTX). Besides this, Lab. No. 1 obtained E values by measuring P- and S-wave velocities. Labs. No. 9 and 10 obtained G values from resonant column (RC) or cyclic torsional test (CTS). Lab. No. 20 fitted the piezoelectric actuator in the top cap, applied P- and S-wave signals, measured the acceleration with accelerometers fitted at the two ends of specimen along the side and obtained G values from shear wave velocity and E values from P-wave velocity. The G values were then calculated from E values ($E=\rho V_P^2$) by

Table 4. Test methods and test conditions

Lab. No.	Apparatus	Test method					Test condition				Remarks
		Acc.	P-wave	RC	CTS	CTX	Dry		Saturated		
							$K=1$	$K=0.5$	$K=1$	$K=0.5$	
1	TX		E				○				V_P by BE
2	TX					E, G			○	○	CTX (undrained), $\nu=0.5$
7	TX					E, G			○	○	p' const CTX
8	TX					E	○				CTX (drained)
9	RC/TS			G	G		○		○		TS, RC
12	RC			G			○	○	○	○	RC
13	TX					E, G	○	○			CTX (drained)
14	TX					E, G			○		CTX (undrained), $\nu=0.5$
20	TX	G	E, G			E, G	○	○			
21	TX					E, G	○	○	○	○	CTX (draine, undrained), $\nu=0.5$
22	TX					E, G			○		CTX (undrained), $\nu=0.5$
23	TX					E, G	○		○		CTX (drained), $\nu=0.25$

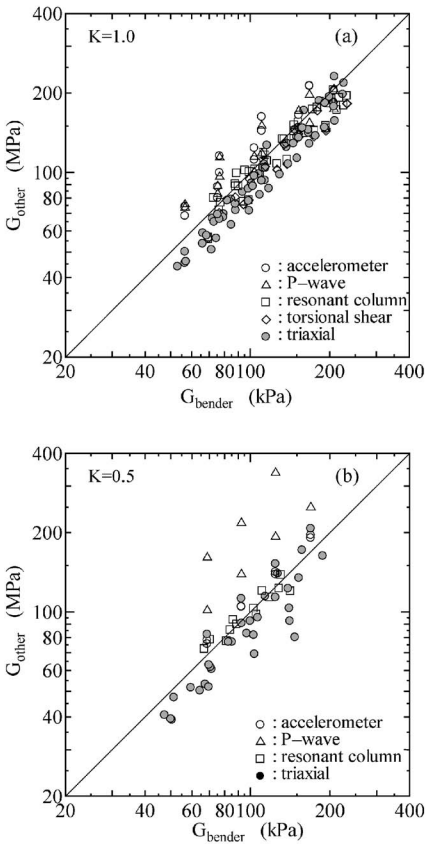

Fig. 39. Comparison of BE and others test results; (a) $K = 1.0$ and (b) $K = 0.5$

assuming Poisson's ratio v. Furthermore, although Lab. No. 23 evaluated the E values from cyclic loadings in the triaxial tests but as the strain level involved was quite large, it was not included in comparison below.

Figure 39 compares G values from BE test (G_{bender}) against those obtained from other type of tests (G_{other}) based upon different consolidation conditions (isotropic or anisotropic). As G values from BE test submitted by different laboratories differed in input frequency as well as the identification method, the following guideline was adopted to obtain single G value:

i) If the results from multiple methods (T.D., C.C. and F.D.) were submitted, the value from T.D. method was selected. If T.D. data was not available, the sequence of selection was in the order of C.C. and F.D.
ii) If the reports were available for square or sine input waves, sine wave was selected.
iii) If data at different frequencies were available within the sine wave, the result obtained by input frequency closest to 10 kHz was selected.
iv) If multiple receiving points were considered for interpretation, the value calculated using S-S method was selected.

It is found from Fig. 39 that G obtained from resonant column test (□ symbols) and torsional shear test (◇ symbols) closely agree with the G values obtained from the BE test. On the other hand, the G from shear wave velocity measured by an accelerometer (○ symbols) and P-waves (△ symbols) showed slightly higher values. The measurement of S- and P-wave arrival points with an accelerometer involves the decision about reading positions, similar to the BE methods described earlier. In the tests, the measurement was taken by considering multiple points, such as initial start-up or the peak point. The calculated G values obviously differed with the reading positions and some of them are identical to the BE results. In addition, G values from triaxial test (● symbols) fall slightly below that of BE tests. The tendency of getting smaller G values from the triaxial test, for which G is calculated from E and v has been recognized from the past parallel tests done so far. The difference existed in both drained triaxial tests, for which v value calculated from the drained tests was used and also for undrained tests, for which v value was simply taken as 0.5.

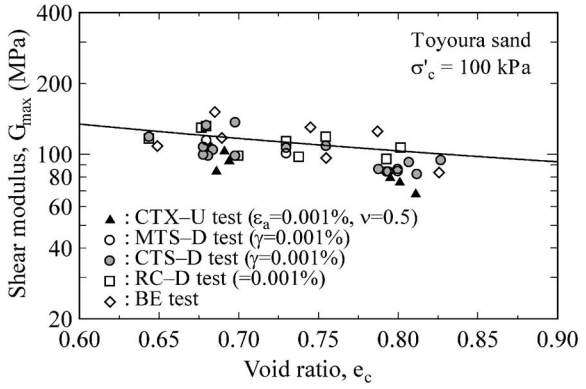

Fig. 40. Last RR test results (modified from Yamashita et al., 2001)

Figure 40 shows the results of the previous round robin test sponsored by TC29 (Yamashita et al., 2001). As compared with BE test, G values obtained from undrained triaxial test are slightly smaller. Some of the factors for such lower values of G from triaxial test could be the effect of bedding error while measuring the axial displacement (Goto et al., 1991), lower B-value and therefore smaller value of Poisson's ratio ($v < 0.5$) at undrained condition (Yamashita et al., 1996), influence of specimen anisotropy (Hoque and Tatsuoka, 1998), the relation between the wave length of the shear wave and particle diameter (Tanaka et al., 2000; Anhdan et al., 2002) and so on. G values, which were evaluated from the tests except BE in this parallel test, fell inside the scatter range indicated by past simultaneous tests and therefore, thought to be more reliable.

PROPOSED BE TEST METHOD

By evaluating the BE test results from 23 institutions from 11 countries, the following standard test procedures for BE testing have been proposed to obtain the most appropriate test results. The test process given below is for a pulse of sine wave as input. Among the results reported this time, the rectangular wave and continuous waves were also adopted other than single sine wave pulse.

However, as the case records were only a few and it was not possible to judge their appropriateness, this report is relevant only with the single sinusoidal wave as an input.

- No clear influence of the difference in bender size, its structure, cantilever length and wiring method was recognized, but the average dimension used by the most laboratories was the width of 10 mm, thickness of 0.5 to 1.0 mm and cantilever length of 5 mm.
- Before starting the test, BE pairs for transmission and reception are made to contact directly and delay time of the whole system as well as the polarity of initial motion need to be verified.
- Frequency of transmitting wave is adjusted so that it becomes equal to the frequency of the receiving wave. Otherwise, multiple input frequencies are used.
- Sampling interval shall be smaller than 1/100th of expected arrival time. In case of very small distance between the benders and required resolution cannot be satisfied, the precision may be increased by using multiple frequencies.
- Voltage resolution shall be more that 1/100th of the largest amplitude of the receiving wave. For example, when largest amplitude is 5 mV, the required resolution becomes 0.05 mV. This value is normally present in the digital oscilloscopes being used presently. When resolution cannot be satisfied, transmission voltage may be increased.
- The same value can be obtained by making use of either of the S-S or P-P or C.C. method of identification so, no specific method is recommended. However, when P-P method or C.C. method is used, frequency of input wave and the receiving wave shall be almost equal. In addition, when C.C. method is used and the 1st wave in the receiving end does not have the largest amplitude, the attention shall be paid not to calculate the arrival time at the location of the maximum amplitude in C.C. function.
- When a test is conducted in a consolidation apparatus that use hard metal container or when the distance between the benders is short, the decision shall be taken relatively by using input waves of multiple frequencies and taking care of using wave length shorter than half the distance between benders.
- Regarding the F.D. method, reliable method for obtaining most appropriate data has not been concluded at present. From the fact that the scatter in F.D. method was quite large in the submitted data, it is quite dangerous to identify the arrival time with only this method.

CONCLUSIONS

The international parallel test for shear modulus evaluation was conducted from 2003 to 2005 by using BEs and Toyoura sand as a sample. Altogether, the participation of 23 laboratories from 11 countries was confirmed. The purpose was to clarify the existing state of evaluation techniques for the BE test and to recommend a standard test procedure for obtaining the most appropriate test results by clarifying the influence of various factors. The following is what could be deduced from the submitted test results:

1) On plotting the entire data reported from the various laboratories, the scatter was found to be rather large. In general, the scatter was large in dry specimens than in the saturated specimens. Similarly, the results from K_0-tests performed in consolidation apparatus had larger scatter as compared to the isotropically consolidated specimens. The reasons for such scatter is not only the difference in identification method but also that some laboratories have evaluated the G value by assuming multiple arrival points in a received wave.
2) Concerning the difference in arrival time identification method, i) the scatter in S-S method is small in comparison with other methods, ii) there is a tendency that P-P and the cross-correlation methods yield relatively small value of G than the S-S method, and iii) it is expected that there is no difference in G value due to saturation condition, i.e., dry or saturated, but larger scatters are associated with dry specimens.
3) When compared with the other test results, G obtained from resonant column and torsional shear tests almost agree with BE test results. On the other hand, G values obtained from triaxial test are slightly smaller as compared to BE test. This tendency agreed with similar parallel tests in the past.
4) The digital data submitted by laboratories was rearranged by using unified identification method. As a result, the following points were noted:
   - If arrival time is identified with S-S method, the scatter in the value of G reduced remarkably as compared with the originally submitted data from each laboratory. However, there still remain large scatter in the data for dry sample and K_0-consolidation sample as compared to the saturated samples and isotropically consolidated samples. A few of the data also deviated from the mean value. For most cases, reading an arrival point in the received wave was quite difficult due to a very low frequency of input wave and low resolution of sampling.
   - The data scatter decreases even if the P-P method is used for interpretation. Variation in wave scatter still remains for dry sample. In addition, in the case of the P-P method, error is easy to occur when low frequency input wave is used.
   - With the C.C. method, frequency of the input wave and the receiving wave is presumed to be equal; so the extent of error is likely to increase whenever the frequency of the input and the receiving wave differs, very similar to the P-P method. It is well noted that slight scatter is found for dry specimens than the saturated ones even with C.C. method.
   - The reason for larger variation in dry specimens is thought to lie on the relatively large noise before

true shear wave signal and the longer reverberation time, among others.

- As one of the methods of F.D. technique, phase cross spectrum was evaluated. In order to obtain appropriate value of G using this method, the following two conditions shall be fulfilled: i) amplitude of the first peak in the receiving wave showing the shear wave arrival shall be the maximum, and ii) the frequency of input shear wave shall be almost equal to the frequency of the first wave at reception.

5) On the basis of the results as described above, standard procedure for BE test has been proposed here to obtain the appropriate test results in the present condition.

ACKNOWLEDGEMENTS

On behalf of TC-29, the authors wish to appreciate the tremendous co-operation of all the laboratories that participated in the international parallel test.

REFERENCES

1) Anhdan, L., Koseki, J. and Sato, T. (2002): Comparison of Young's moduli of dense sand and gravel measured by dynamic and static methods, *Geotechnical Testing Journal*, ASTM, **25**(4), 349–368.
2) Arroyo, M., Muir Wood, D., Greening, P. D., Medina, L. and Rio, J. (2006): Effects of sample size on bender-based axial G_0 measurements, *Gèotechnique*, **56**(1), 39–52.
3) Blewett, J., Blewett, I. J. and Woodward, P. K. (1999): Measurement of shear wave velocity using phase sensitive detection techniques, *Canadian Geotechnical Journal*, **36**, 934–939.
4) Brignoli, E. G. M., Gotti, M. and Stokoe, K. H., II (1996): Measurement of shear waves in laboratory specimens by means of piezoelectric transducers, *Geotechnical Testing Journal*, ASTM, **19**(4), 384–397.
5) Dyvik, R. and Madshus, C. (1985): Laboratory measurement of G_{max} using bender elements, *Advances in the Art of Testing Soils under Cyclic Conditions*, ASCE, 186–196.
6) Goto, S., Tatsuoka, F., Shibuya, S., Kim, Y.-S. and Sato, T. (1991): A simple gauge for local small strain measurements in the laboratory, *Soils and Foundations*, **31**(1), 169–180.
7) Greening, P. D. and Nash, A. F. T. (2004): Frequency domain determination of G_0 using bender elements, *Geotechnical Testing Journal*, ASTM, **27**(3), 288–294.
8) Hoque, E. and Tatsuoka, F. (1998): Anisotropy in elastic deformation of granular materials, *Soils and Foundations*, **38**(1), 163–179.
9) Iwasaki, T. and Tatsuoka, F. (1997): Effect of grain size and grading on dynamic shear moduli of sands, *Soils and Foundations*, **17**(3), 19–35.
10) Japanese Geotechnical Society (2000): JGS 0542-2000 Method for cyclic triaxial test to determine deformation properties of geomaterials, *Standards of Japanese Geotechnical Society for Laboratory Shear Test*, 62–72.
11) Jovičić, V., Coop, M. R. and Simić, M. (1996): Objective criteria for determining G_{max} from bender element tests, *Gèotechnique*, **46**(2), 357–362.
12) Kawaguchi, T., Mitachi, T. and Shibuya, S. (2001): Evaluation of shear wave travel time in laboratory bender element test, *Proc. 15th ICSMGE*, **1**, 155–158.
13) Lings, M. L. and Greening, P. D. (2001): A novel bender/extender element for soil testing, *Gèotechnique*, **51**(8), 713–717.
14) Mancuso, C., Simonelli, A. L. and Vinale, F. (1989): Numerical analysis of in situ S-wave measurements, *Proc. 12th ICSMFE*, Rio de Janeiro, **3**, 277–280.
15) Miura, S., Toki, S. and Tatsuoka, F. (1994): Cyclic undrained triaxial behaviour of sand by a cooperative test program in Japan, *Dynamic Geotechnical Testing*, **2**, ASTM STP 1213, 246–260.
16) Roesler, S. K. (1979): Anisotropic shear modulus due to stress anisotropy, *Journal of Geotechnical Engineering*, ASCE, **105**(7), 871–880.
17) Stokoe, K. H. II, Hwang, S. K., Lee, N. K. J. and Andrus, R. D. (1995): Effect of various parameters on the stiffness and damping of soils at small to medium strains, Keynote lecture, *Proc. 1st International Conference on Pre-failure Deformation of Geomaterials*, Sapporo, Balkema, 785–816.
18) Tanaka, Y., Kudo, K., Nishi, K., Okamoto, T., Kataoka, T. and Ueshima, T. (2000): Small strain characteristics of soils in Hualian, Taiwan, *Soils and Foundations*, **40**(3), 111–125.
19) Tatsuoka, F., Toki, S., Miura, S., Kato, H., Okamoto, M., Yamada, S., Yasuda, S. and Tanizawa, F. (1986): Some factors affecting cyclic undrained triaxial strength of sand, *Soils and Foundations*, **26**(3), 99–116.
20) Tatsuoka, F., Shibuya, S. and Kuwano, E. (2001): *Advanced Laboratory Stress-Strain Testing of Geomaterials*, Balkema.
21) Toki, S., Tatsuoka, F., Miura, S., Yoshimi, Y., Yasuda, S. and Makihara, Y. (1986): Cyclic undrained triaxial strength of sand by a cooperative test program, *Soils and Foundations*, **26**(3), 117–156.
22) Toki, S., Shibuya, S. and Yamashita, S. (1995): Standardization of laboratory test methods to determine the cyclic deformation properties of geomaterials in Japan, *Proc. 1st International Conference on Pre-failure Deformation of Geomaterials*, Sapporo, Balkema, 741–789.
23) Viggiani, G. and Atkinson, J. H. (1995): Interpretation of bender element test, *Gèotechnique*, **45**(1), 149–154.
24) Yamashita, S., Toki, S. and Suzuki, S. (1996): Effect of membrane penetration on modulus and Poisson's ratio for undrained cyclic triaxial conditions, *Soils and Foundations*, **36**(4), 127–133.
25) Yamashita, S., Kohata, H., Kawaguchi, T. and Shibuya, S. (2001): International round robin test organized by TC29, *Advanced Laboratory Stress Strain Testing of Geomaterials*, Balkema, 65–110.

APPENDIX: STANDARD TEST SPECIFICATION FOR INTERNATIONAL PARALLEL TEST ON THE MEASUREMENT OF G_{max} USING BENDER ELEMENTS BY TC-29

1 Test material and testing apparatus
- The test material is Toyoura sand.
- 5 kg of Toyoura sand will be distributed to each laboratory.
- Testing apparatus is triaxial, consolidometer, resonant column etc. equipped with bender elements.

2 Sample preparation
- Specimens which will have D_r equal to 50 and 80% (dry densities ρ_d equal to 1.465 and 1.553 g/cm^3) as determined at initial stress condition ($\sigma'_v = 25$ kPa) are prepared by the air-pluviation method; air-dried sand is poured from a copper nozzle with a rectangular inner cross-section of 1.5 mm × 15.0 mm, while maintaining a constant drop-height throughout the preparation.
- The final top surface of specimen is made level and smooth by scraping with a thin plate having a straight edge.
- These nozzles will be produced by the Japanese

domestic committee of TC-29, and will be distributed to the members of TC-29.

3 Specimen set-up (except for consolidometer)
- Before the mold is disassembled, a partial vacuum of 10 kPa is applied to the specimen, while the loading piston is unclamped.
- Subsequently, the mold is dismantled, and then the vacuum is raised to 25 kPa while ensuring that the specimen can deform freely both in the axial and lateral directions.
- Then, initial specimen height and diameter are measured, and the results are reported.
- The partial vacuum is replaced with a cell pressure of 25 kPa while keeping the effective stress constant throughout the procedure.

4 Consolidation and Measurements of shear wave velocity
- Sample conditions in testing are dry or fully saturated.
- In the case of saturated specimen, the specimen is saturated using any of or a combination of appropriate saturation techniques. A back pressure of 100 kPa is applied.
- Consolidation condition is isotropic or anisotropic ($K=0.5$ or K_0 (consolidometer)), and the consolidation stresses are $\sigma'_v=50$, 100, 200 and 400 kPa (*see* Fig. A-1). e.g.; in the case of $K=0.5$, $\sigma'_v=50$, 100, 200, 400 kPa ($\sigma'_h=25$, 50, 100, 200 kPa).

4.1 Isotropic consolidation

a) Keeping the isotropic stress state in the drained condition, increase the confining stress to the next isotropic stress state ($\sigma'_c=50$, 100, 200 or 400 kPa) in one or two minutes as shown in Fig. A-1.
b) Consolidate 10 minutes on each stress state (open circle marks in Fig. A-1).
c) Measure the changes in the height and volume of the specimen.
d) Measure the shear wave velocities using the bender element.
e) Measure the secant stiffness from stress-strain curve at small strains (less than 0.001%) by applying monotonic or cyclic loading in the drained and/or undrained conditions when possible.
f) Measure the changes in the height and volume of the specimen after the measurement of V_s and/or stiffness.
g) Repeat the processes a) to f) until the final stress state ($\sigma'_c=400$ kPa) is reached.

4.2 Anisotropic consolidation ($K=0.5$)

a) In the drained condition, apply the vertical stress up to 50 kPa ($\sigma'_h=25$ kPa and $K=0.5$).
b) Consolidate 10 minutes on $K=0.5$ stress state (solid circle marks in Fig. A-1).
c) Measure the changes in the height and volume of the specimen.
d) Measure the shear wave velocities using the bender element.
e) Measure the secant stiffness from stress-strain curve at small strains (less than 0.001%) by applying monotonic or cyclic loading in the drained and/or undrained conditions when possible.
f) Measure the changes in the height and volume of the specimen after the measurement of V_s and/or stiffness.
g) Increase the horizontal and vertical stresses step by step until next anisotropic stress state (solid circle marks in Fig. A-1) in one or two minutes on each step. The increment of horizontal and vertical stresses, $\Delta\sigma'_h$, σ'_v are 25 and 50 kPa, respectively.
h) Repeat the processes b) to g) until the final stress state ($\sigma'_v=400$ kPa and $\sigma'_h=200$ kPa) is reached.

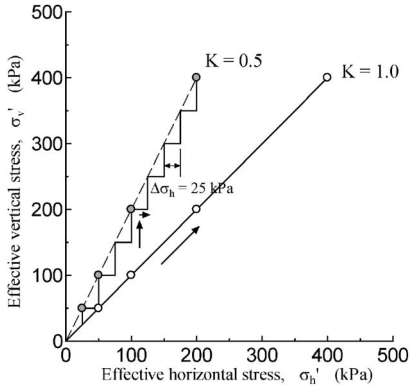

Fig. A-1. Stress path at consolidation

4.3 K_0 consolidation (consolidometer)

a) In the drained condition, increase the vertical stress to the next stress state ($\sigma'_v=50$, 100, 200 or 400 kPa) in one or two minutes.
b) Consolidate 10 minutes on each stress state.
c) Measure the changes in the height of the specimen.
d) Measure the shear wave velocities using the bender element.
e) Measure the changes in the height of the specimen after the measurement of V_s.
f) Repeat the processes a) to e) until the final stress state ($\sigma'_v=400$ kPa) is reached.

5 Report

1) Outline of the test apparatus used.
2) Details of benders employed (e.g., maker, shape, dimension, thickness and material of Piezoelectric Ceramics, mounting, the tip-to-tip distance, electrical connections (series or parallel etc.). Schematic figure indicated dimension of cap and/or pedestal with bender elements.
3) Fill up the items listed in Form attached.
4) Input and received wave record in digital data or hardcopy of screen. Sampling frequency and whether filter used or not.
5) Determination of arrival time (V_s), special treatment (cross correlation, self monitoring, etc.).
6) Strain rate of monotonic loading, and/or frequency and number of loading cycle of cyclic loading.
7) Stress and strain records on monotonic and/or cyclic loadings in digital data.
8) Any deviations from the procedure outlined in this specification.